

PARAMETRIZATION OF ELECTRON CLOUD BUILDUP MODELS

A. M. Furman, L. Mether¹, T. Pieloni, L. Sabato³, M. Seidel^{2,3}

¹European Organization for Nuclear Research, Geneva, Switzerland

²Paul Scherrer Institute, Villigen, Switzerland

³École Polytechnique Fédérale de Lausanne, Lausanne, Switzerland

Abstract

The buildup of electron clouds (EC) within the beam chamber limits machine performance by causing heating, beam instabilities, and other undesirable effects. Macroparticle simulations show that EC density can be modelled as a smooth curve with superimposed oscillations of a frequency corresponding to the beam bunch spacing. The saturation density and rate of electron cloud buildup can be linked to the best-fit parameters of the mathematical model chosen for the smooth curve. Our work investigates the dependence of each curve parameter on the simulation parameters, looking to reduce the number of simulations necessary to gain a complete picture of EC buildup per machine configuration. Correlations among the parameters can be utilized to formulate predictions using fewer data points.

INTRODUCTION

Understanding electron cloud (EC) buildup in proposed particle accelerators is a critical step in the design process. The buildup process is simulated using a software package such as PyECLOUD [1] which takes as input the machine and beam parameters, and outputs the state of the EC over time in a two-dimensional cross-section of the machine. PyECLOUD simulations, while robust and well-tested, are computationally costly. Especially when considering new accelerator designs, such as the FCC (Future Circular Collider) at CERN, evaluating the full range of EC behaviour requires sweeps across many parameters at fine resolution, necessitating thousands of simulations.

This paper outlines a method for reducing the number of simulations necessary to understand EC behaviour by parametrizing the results of PyECLOUD simulations using a semi-analytical model for EC buildup based on the work of M. A. Furman [2]¹. A useful model should describe: first, whether or not the EC will build up over time, second, the saturation density of the EC (how dense it can become before it stops building up more), and finally how quickly the saturation density is achieved. In addition, different kinds of magnetic fields as well as photoelectron emission complicate the dynamics of the EC.

SEMI-ANALYTICAL MODEL

Furman derives an ordinary differential equation model for the EC linear density as a function of time, under the assumption of a bunched beam.

$$\frac{dy}{dx} = \alpha + \beta (y_c - y) y, \quad (1)$$

where $x = t/t_b$ is the bunch passage number and $y = \lambda_e/I_{avg}$ is the EC line density scaled by the average bunch intensity (over one t_b). The three parameters are:

- y_c : The critical (saturation) EC density.
- α : The number of photoelectrons generated per t_b .
- β : Related to the rate of accumulation of the EC.

Furman [2] solves Eq. (1) with the initial condition $y(0) = 0$ (no initial EC) and $\alpha > 0$ (photoemission is present) with:

$$y(x) = \frac{-y_+ y_- (e^{\beta(y_+ - y_-)x} - 1)}{y_+ - y_- e^{\beta(y_+ - y_-)x}}, \quad (2)$$

with $y_{\pm} = \frac{1}{2} \left(y_c \pm \sqrt{y_c^2 + \frac{4\alpha}{\beta}} \right)$.

This paper produces two additional solutions to Eq. (1). First, considering an initial EC $y(0) = y_0 > 0$, and no photoemission $\alpha = 0$, the solution is:

$$y(x) = \frac{y_0 y_c e^{\beta y_c x}}{y_c + y_0 (e^{\beta y_c x} - 1)}. \quad (3)$$

Second, considering both an initial EC $y(0) = y_0 > 0$, and photoemission $\alpha > 0$:

$$y(x) = \frac{y_c}{2} + \sqrt{\frac{y_c^2}{4} + \frac{\alpha}{\beta}} \tanh \left(\frac{x}{2} \sqrt{4\alpha\beta + (y_c\beta)^2} - \phi \right), \quad (4)$$

with $\phi = \arctan \left((y_c - 2y_0) \sqrt{\frac{\beta}{4\alpha + y_c^2\beta}} \right)$. It can be shown that Eq. (4) reduces to Eq. (2) or Eq. (3) under the corresponding conditions. Note that in Eq. (3), $\lim_{x \rightarrow \infty} y(x) = y_c$, but in Eqs. (2) and (4), the limit is $\frac{y_c}{2} + \sqrt{\frac{y_c^2}{4} + \frac{\alpha}{\beta}} = y_+$.

The inflection point of Eq. (3), where $y(x_\tau) = y_c/2$, occurs at $x_\tau = \frac{1}{y_c\beta} \ln \left(\frac{y_c}{y_0} - 1 \right)$, as marked (red X) in Fig. 1. For Eq. (4), it occurs at $x_\tau = \frac{2\phi}{\sqrt{4\alpha\beta + (y_c\beta)^2}}$, as marked in Fig. 2. The inflection points provide a characteristic growth time (in units of the bunch spacing t_b) for the EC.

¹ No relation to the author of this work, A. M. Furman.

This work was performed under the auspices of, and with support from, the Swiss Accelerator Research and Technology (CHART) program (www.chart.ch).

All three models can be fit to PyECLLOUD simulations to obtain (α, β, y_c) . It is important to state that all models derived from Eq. (1) only capture EC buildup on the time scale of individual bunch passages t_b , since the form of the equation is obtained by approximating the instantaneous intensity by I_{avg} . Within each t_b , the electron cloud density undergoes oscillations that may possibly be described using an extended version of Eq. (1) that is not further discussed here. All curve fits are done on one sample per t_b , taking the average electron cloud density within $(nt_b, (n+1)t_b)$.

CURVE FITTING

Many parameters can influence EC buildup, but bunch intensity I and the secondary electron yield (SEY) are among the most important. The SEY $\delta(E)$ determines how many secondary electrons are produced for each primary electron which hits the beam chamber wall with an energy E , and the function has a maximum δ_{max} at the energy E_{max} [3]. Together with the type and strength of magnetic field B , sweeping the values of I and δ_{max} characterizes EC buildup, since increasing I is often the design goal of the machine and δ_{max} varies both with time and across different materials.

Figure 1 shows the $N_e(t)$ output of a PyECLLOUD simulation. The gray background (“All Data”) shows the extent of the EC density oscillations within each t_b interval, with the black points (“Fitting Data”) being the average values used for curve fitting. Here, no photoemission of electrons was simulated, so $\alpha = 0$ and thus Eq. (3) is used.

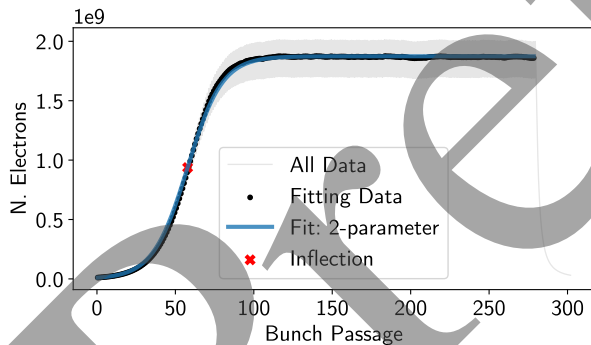


Figure 1: PyECLLOUD simulation for a drift section ($B = 0$), with $I = 9.89 \times 10^{10}$ ppb, $\delta_{max} = 1.4$, no photoemission.

Figure 2 shows the same configuration as Fig. 1, but now including constant uniform photoemission of 10^{-3} electrons per beam particle per unit length along the beam chamber. Two different ways of finding the α , β , and y_c parameters for Eq. (4) are shown. The blue line (“Fit: 3-parameter”) shows Eq. (4) fit directly to the data in Fig. 2. The orange line (“Fit: from non-pe”) line shows Eq. (4) plotted with β and y_c values taken from Fig. 1, and α inferred using the final data point. The two fits in the figure show it is possible to infer the full model in Eq. (4) from a computationally less costly simulation without photoemission as long as there is a way to predict α , the difficulty of which is discussed in more detail in the next section.

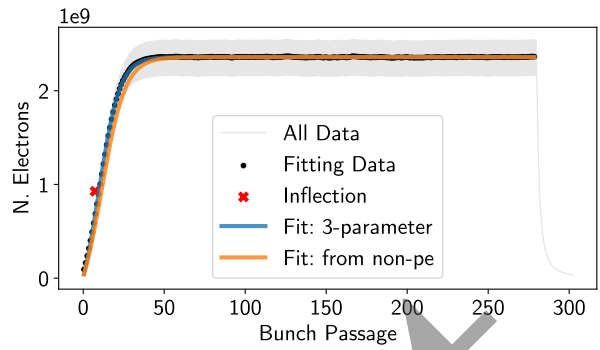


Figure 2: PyECLLOUD simulation for a drift section ($B = 0$), $I = 9.89 \times 10^{10}$ ppb, $\delta_{max} = 1.4$, with photoemission.

PARAMETER PREDICTION

The dependence of α , β , and y_c on intensity, SEY, magnetic field, and other simulation parameters is of great interest. If a clear trend exists, even without a full analytical model, a smaller number of simulations can be extrapolated to gain an understanding of a complete parameter sweep.

Starting with simulations where $\alpha = 0$ (no photoemission), Fig. 3 shows a linear trend between the SEY δ_{max} input and the y_c parameter, coloured by bunch intensity.

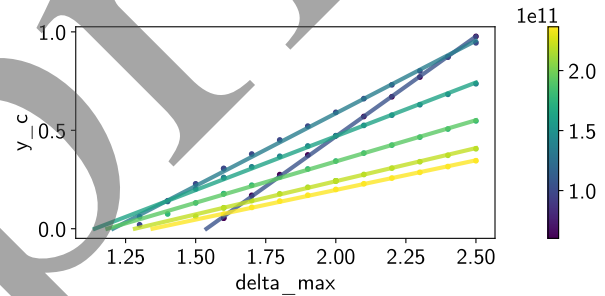


Figure 3: Linear predictive models $y_c(\delta_{max})$ (lines) from Eq. (3) fits (dots), coloured by bunch intensity I ; $B = 0$.

Similarly, Fig. 4 shows the relationship between the SEY δ_{max} input and the β parameter, coloured by bunch intensity.

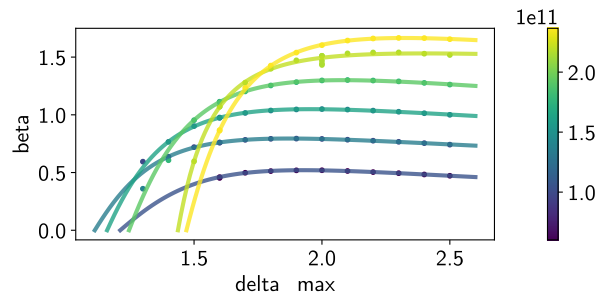


Figure 4: Predictive models $\beta(\delta_{max})$ (curves) from Eq. (3) fits (dots), coloured by bunch intensity I ; $B = 0$.

The predictive model for β as shown in Fig. 4 is not linear:

$$\beta(\delta_{max}) = \frac{ABs(\delta_{max} - \delta_0)}{s - 1 + (A(\delta_{max} - \delta_0))^s}. \quad (5)$$

The form of Eq. (5) is inspired by the function which defines the energy dependence of the secondary electron emission

yield [3, 4], where $A = 1/E_{\max}$, $B = \delta_{\max}$, $s = 1.35$, and $\delta_0 = 0$. Whether this form is coincidental or physically significant is a topic for further study.

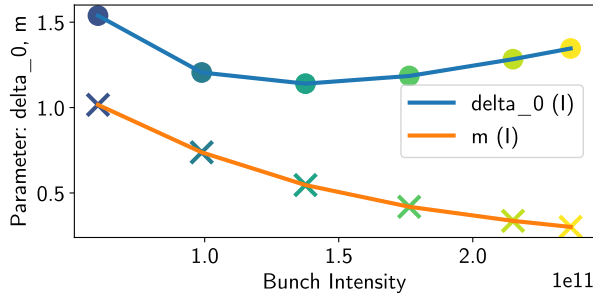


Figure 5: The parameters δ_0 (intercept) and m (slope) that describe the lines in Fig. 3; each I corresponds to one line.

Each line in Fig. 3 corresponds to two values: δ_0 and m , representing the intercept (the δ_{\max} at which no EC buildup would occur) and slope of the line. If δ_0 and m exhibit a clear trend with respect to intensity, then we can combine both models: $y_c(\delta_{\max}, I) = m(I) \cdot (\delta_{\max} - \delta_0(I))$. Figure 5 shows that $m(I)$ (dots) and $\delta_0(I)$ (crosses) both exhibit polynomial trends with respect to the bunch intensity. A lower δ_0 value means that the multipacting regime [1, p. 19] – where enough secondary electrons are emitted to accumulate the EC – occurs at a lower δ_{\max} . Notably, the lowest δ_0 does not occur for the highest intensity, rather, it exhibits a minimum at an intermediate “critical intensity.”

Figures 3, 4, and 5 are based on fits of Eq. (3), and correspond to simulations without photoemission like the example in Fig. 1. In the simulations, photoemission is added via the parameter $k_{pe,st}$ the number of photoelectrons generated per beam particle per unit length [1, p. 31]. Furman defines α as the number of photoelectrons generated over one bunch passage t_b , so the two quantities should be correlated as

$$\alpha = ct_b \cdot k_{pe,st}, \quad (6)$$

where the velocity of the beam is approximated by the speed of light c . Figure 6 compares the prediction of Eq. (6) to the fit value of α . We observe a large discrepancy between the two across $k_{pe,st}$ values and bunch intensities, because $k_{pe,st}$ determines the number of photoelectrons emitted but not if and how they contribute to the EC. Some simulation configurations are more sensitive to a change in the photoelectron emission rate than others – the fit α value measures the response of the EC to photoemission.

CONCLUSION AND FURTHER WORK

Using the semi-analytical approach inspired by Furman [2], an expanded model (Eqs. (3) and (4)) provides three parameters α , β , and y_c for describing the EC buildup. These parameters can be predicted based on the simulation inputs, especially the SEY δ_{\max} and bunch intensity. Using these models reduces the amount of simulations necessary to characterize the EC behaviour of a given machine configuration.

The analysis presented here is focused on drift sections ($B = 0$) because the Furman model [2] does not take into

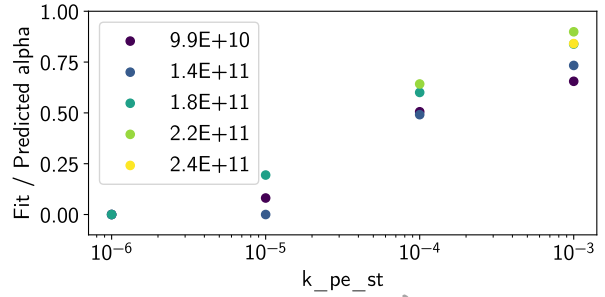


Figure 6: Ratio of fit over predicted α values as a function of $k_{pe,st}$ and I ; $B = 0$, $\delta_{\max} = 1.4$.

account any magnetic field effects on the EC. Fig. 7 shows fits for the drift section (equivalent to Fig. 1) as well as for a dipole, quadrupole, and sextupole field.

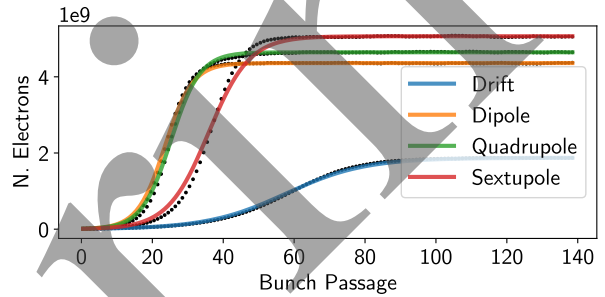


Figure 7: Equivalent simulations to Fig. 1 with different magnets, showing data (dots) and Eq. (3) fits (lines).

In all cases, the presence of a magnetic field increases y_c , the saturation density of the EC, due to the trapping effect of the field on the electrons. There is also a discrepancy between the fit of Eq. (3) and the actual data points during the growth phase where the EC density is increasing: the presence of a magnetic field appears to increase the growth rate, but not the saturation density. A logical extension of the model presented here would include additional parameters for capturing the effects of differing magnetic field types and intensities. In the long run, a tool alongside PyECLOUD is envisioned that would fill in parameter sweeps using the predictive models described here.

REFERENCES

- [1] G. Iadarola, E. Belli, K.S.B. Li, L. Mether, A. Romano, and G. Rumolo, “Evolution of Python Tools for the Simulation of Electron Cloud Effects”, in *Proc. IPAC’17*, Copenhagen, Denmark, pp. 3803–3806, May 2017. doi:10.18429/JACoW-IPAC2017-THPAB043
- [2] M. A. Furman, “Electron-cloud build-up: theory and data”, *Lawrence Berkeley National Laboratory*, 2011. LBNL-4504E/CBP-872
- [3] G. Iadarola, “Electron Cloud Studies for CERN Particle Accelerators and simulation Code Development”, Ph.D. thesis, Naples U., Mar. 2014. CERN-THESIS-2014-047
- [4] M. A. Furman, “The Electron-Cloud Effect in the Arcs of the LHC”, CERN, Geneva, Rep., 1998. cds.cern.ch/record/356436